Published in final edited form as:
J Neurochem. 2010 April ; 113(1): 42–53. doi:10.1111/j.1471-4159.2009.06529.x.

Regulation of stargazin synaptic trafficking by C-terminal PDZ ligand phosphorylation in bidirectional synaptic plasticity

Emma L.A. Stein[1] and **Dane M. Chetkovich**[1,2]

[1]Davee Department of Neurology and Clinical Neurosciences, Feinberg School of Medicine, Northwestern University, Chicago, Illinois 60611

[2]Department of Physiology, Feinberg School of Medicine, Northwestern University, Chicago, Illinois 60611

Abstract

Stargazin is a transmembrane AMPA receptor regulatory protein (TARP) that controls the surface and synaptic expression of AMPA-type glutamate receptors (AMPARs). Synaptic anchoring of AMPARs is influenced by the interaction between stargazin's C-terminal PDZ ligand and the synaptic scaffolding protein PSD-95. Phosphorylation of the stargazin PDZ ligand by PKA disrupts stargazin's interaction with PSD-95, but whether this phosphorylation plays a role in activity-dependent regulation of stargazin/AMPAR synaptic trafficking is unknown. Here, we show that stargazin is phosphorylated within the PDZ ligand at threonine residue 321 (T321) by MAP kinases (MAPKs) as well as PKA. By expressing constructs that selectively block T321 phosphorylation by either PKA or MAPKs, we show that stargazin T321 phosphorylation is required for activity-dependent changes in stargazin synaptic clustering in dissociated rat hippocampal neuron cultures. Specifically, we find that mutations that block stargazin T321 phosphorylation by PKA prevent activity-dependent increases in stargazin synaptic clustering, whereas a point mutant that blocks MAPK phosphorylation of T321 prevents activity-dependent decreases in stargazin synaptic clustering. Taken together, our studies implicate phosphorylation of stargazin T321 by PKA and MAPKs in bidirectional control of stargazin/AMPAR synaptic clustering during synaptic plasticity.

Keywords

Stargazin; PDZ ligand phosphorylation; LTP; LTD; Cultured neurons; AMPA receptor trafficking

Introduction

The number of α-amino-3-hydroxy-5-methyl-4-isoxazolepropionic acid (AMPA)-type glutamate receptors present at neuronal excitatory synapses is dynamically regulated to control the strength of synaptic connections. Alterations in synaptic AMPAR content are largely responsible for changes in synaptic efficacy that underlie hippocampal long-term

Corresponding Author: Dane M. Chetkovich, MD, PhD, Davee Department of Neurology and Clinical Neuroscience, Feinberg School of Medicine, Northwestern University, 303 East Chicago Avenue, Ward 10-201, Chicago, IL 60611-3008, Office: 312-503-4362, Fax: 312-503-0872, d-chetkovich@northwestern.edu.

potentiation (LTP) and long-term depression (LTD) (Carroll et al. 1999; Lüscher et al. 1999; Lüthi et al. 1999; Shi et al. 1999; Man et al. 2000; Nosyreva and Huber 2005). The mechanisms governing activity-dependent synaptic trafficking of AMPARs are an area of intense study, and have focused largely on the AMPAR GluR1-4 subunit C-terminal domains (CTDs) and their interacting proteins (Passafaro et al. 2001; Shi et al. 2001; Piccini and Malinow 2002), but recent studies have brought into question the importance of the role of GluR CTDs in regulating AMPAR trafficking (States et al. 2008; Lu et al. 2009). Although there is an important role for transmembrane AMPAR regulatory proteins (TARPs) in controlling AMPAR cell surface and synaptic targeting (Bats et al. 2007; Ziff 2007), little is known about the role of TARP-mediated AMPAR trafficking in synaptic plasticity.

Stargazin, the prototypical member of the TARP family of AMPAR auxiliary subunits (Tomita et al. 2003; Vandenberghe et al. 2005; Nicoll et al. 2006), contains a type-I postsynaptic density-95 (PSD-95)/Discs large (Dlg)/zona occludens-1 (ZO-1) (PDZ)-binding motif in its extreme C-terminus. The stargazin PDZ ligand interacts with the synaptic scaffolding protein, PSD-95, and is required for stargazin and AMPAR synaptic clustering (Chen et al. 2000). Furthermore, interaction between stargazin and PSD-95 controls the number of AMPARs at synapses (Schnell et al. 2002), and stabilizes laterally-diffusing AMPARs at synaptic PSD-95 clusters (Bats et al. 2007).

The interaction between stargazin and PSD-95 is disrupted by phosphorylation of a critical threonine residue (T321) in stargazin's PDZ ligand by PKA (Chetkovich et al. 2002; Choi et al. 2002). Under basal conditions, stargazin phosphorylated at T321 is present in the brain, but as opposed to non-phosphorylated stargazin is not enriched in the postsynaptic density (PSD) (Choi et al. 2002). Furthermore, in hippocampal neuron cultures, AMPARs are dissociated from synapses by overexpression of an engineered stargazin protein harboring a mutation that mimics PDZ ligand phosphorylation (Chetkovich et al. 2002). Taken together, these prior findings implicate stargazin PDZ ligand phosphorylation in regulating stargazin/AMPAR synaptic anchoring, wherein phosphorylation facilitates dissociation of stargazin/AMPARs from synapses.

In the present study we show that, in addition to PKA, T321 is phosphorylated by ERK2 and p38 MAPK, but not by CaMKII or PKC. In dissociated rat hippocampal neuron cultures, we find that stargazin synaptic clustering is dynamically regulated by chemically-induced forms of LTP (cLTP) and LTD (cLTD). Preventing stargazin PDZ ligand phosphorylation by PKA blocks the cLTP-induced increase in stargazin synaptic clustering. Surprisingly, blocking MAPK-mediated phosphorylation of the stargazin PDZ ligand prevented cLTD-induced decrease in stargazin synaptic clustering. Our findings suggest that stargazin is phosphorylated at T321 by either PKA or MAPKs under different cellular conditions, and that stargazin PDZ ligand phosphorylation plays an important role in controlling the synaptic anchoring of stargazin and associated AMPARs in synaptic plasticity.

Experimental Procedures

All animal experiments were performed according to protocols approved by the Northwestern University Institutional Animal Care and Use Committee.

Antibodies

Guinea pig α-stargazin was produced using a thioredoxin-fusion protein for stargazin(204-323) as antigen (Supplemental Figure S1). Rabbit polyclonal antibodies were made against peptides for stargazin (CQKDSKDSLHANTAN) and stargazin phosphorylated at T321 (CANTANRRTpTPV) (Chetkovich et al. 2002). The rabbit polyclonal antibodies were purified on affinity columns containing the immunizing antigen (Supplemental Figures S1-S2). Other antibodies used include mouse monoclonal antibody against PSD-95 (clone K28/43, NeuroMab; www.neuromab.org) and guinea pig α-green fluorescent protein (GFP) (El-Husseini et al. 2000).

cDNA cloning and mutagenesis

The plasmids encoding full-length stargazin and stargazin Δ4 (Δ319-323), T321E, and R318,319A were described previously (Chen et al. 2000; Chetkovich et al. 2002). GW1-stargazin P322A and pGEX-4T1 (Amersham) plasmids encoding the last 40 amino acids of stargazin's C-terminal tail (stargazin c40) with wild type, Δ4, R318,319A, and P322A mutations were created by PCR using standard methods. The proper DNA sequences were verified for all plasmids prior to use.

Purification of GST-fusion proteins

cDNA encoding the last 40aa of stargazin's C-terminal tail as a GST-fusion protein (pGEX 4t-1 vector, GE Life Sciences) was transformed into bacteria (BL21, Stratagene). Bacterial cultures were grown in Overnight Express Autoinduction Media (Novagen). Bacterial pellets were lysed using BugBuster Master Mix and fusion proteins were affinity purified using on columns containing GST-Bind resin according to manufacturer's protols (Novagen). After elution in glutathione-containing Tris-buffered saline (pH 9.0), fusion proteins were dialyzed in PBS. Protein concentration was determined using the Bradford method.

In vitro phosphorylation assays

Purified GST fusion proteins (10μg) were mixed with purified protein kinase [40-50U PKA, CaMKII, ERK2 (NEB), PKC (Biosource), or p38 MAPK (Biosource or Millipore)] on ice in a final volume of 40μL containing reaction buffer (as specified by manufacturer for each kinase). Reactions were started by the addition of 200μM ATP and incubated for 30 min at 30°C. Reactions were stopped by the addition of ice-cold SDS stop solution, and boiled for 2 min.

Western Blotting

Protein extracts were resolved by SDS-PAGE and transferred to PVDF membranes (Millipore). After blocking 30min in 5% nonfat dry milk and 0.1% Tween-20 in TBS

(TBST-milk), blots were incubated with primary antibody diluted in blocking buffer for 1 hr at room temperature (RT). Blots were washed 3 times for 10 min each with TBST, and appropriate HRP-conjugated secondary antibody (Amersham α-rabbit or α-mouse HRP, 1:10,000; or Sigma α-guinea pig HRP 1:5000) was added in blocking buffer and incubated 1hr at RT. Results were visualized using Supersignal West Pico chemiluminescence (Pierce).

Cell cultures

COS-7 cells (ATCC) were plated on tissue culture-treated 10cm petri dishes for biochemical experiments or 1cm round glass coverslips for immunostaining. Cells were cultured in Dulbecco's Modified Eagle Medium (DMEM; Invitrogen) containing 10% fetal bovine serum (Invitrogen). 24 hr after plating, cells were transfected using Polyfect reagent (Qiagen) according to the manufacturer's protocols. 24-48 hr after transfection, cells were harvested for biochemical experiments or fixed in 4% PFA in PBS and processed for immunostaining as described below. For co-immunoprecipitation (co-IP) experiments, COS-7 cells on 10cm Petri dishes were washed and scraped into 500μL PBS containing 1mM EDTA (PBSE) plus protease inhibitors (10μg/mL each aprotinin and leupeptin). After pelleting by centrifugation, the cells were lysed in 500μL buffer [containing in mM: 50 Tris-HCl pH 7.4, 150 NaCl, 1 EDTA, 1 EGTA; 1% Triton X-100, with 10μg/ml each aprotinin and leupeptin and 1mM PMSF (Sigma); TEEN-Tx] and incubated at 4°C for 40 min with gentle rocking. Cell debris was removed by centrifugation of lysates for 10min at 16,000 × *g*. 50μL of lysate was reserved for co-IP input samples. 2.5μL of rabbit anti-stargazin antibody was added to the remaining lysate, and samples were gently rotated overnight at 4°C. 50μL of a 50% slurry of protein A sepharose beads (Sigma) were then added and samples were rotated at 4°C for 2 hr. The beads were pelleted by brief centrifugation and washed extensively with TEEN-Tx, then resuspended in 50μL TEEN-Tx. 50μL of 2x SDS-PAGE protein loading buffer was added to input and IP samples, which were boiled for 2 min before loading equal volumes of each sample on SDS-PAGE gels. Western blotting was performed as described above.

Neuronal culture and transfection

Dissociated hippocampal neurons from E18 rat pups were plated at a density of about 1200/mm^2 on 1cm round glass coverslips coated with poly-D-lysine (Sigma; 0.1mg/mL in 0.1M borate buffer, pH 8.5) in plating media (10% fetal bovine serum in Neurobasal media supplemented with B27; Invitrogen) in each well of a 24-well plate. After 1 hr, plating media was replaced with Neurobasal media supplemented with B27. Beginning on day 4 in vitro (DIV 4), cultures were fed twice weekly by replacing half of the used media with fresh Neurobasal-B27 containing 200μM DL-APV (Tocris). Hippocampal neurons were transfected on DIV 20-22 using Lipofectamine 2000 reagent (Invitrogen) using the following protocol: For each four wells of neurons, 8-12μg of DNA (at a ratio of 3μg stargazin:1μg GFP DNA) was mixed with 12μL of Lipofectamine 2000 in 200μL of DMEM containing 1mM sterile HEPES buffer (pH 7.0; CellGro). The DNA-Lipofectamine 2000 mixture was incubated for 20 min at 37°C. 50μL of the mixture was added to each of the four wells and incubated for 4 hr at 37°C, after which the coverslips were transferred to a mixture of 50% used and 50% fresh feeding media.

APV withdrawal-induced cLTP

APV withdrawal experiments were performed 2-3 days after transfection (at DIV 22-25). Briefly, coverslips were transferred to artificial cerebrospinal fluid [aCSF, containing (in mM): 125 NaCl, 2.5 KCl, 26.2 $NaHCO_3$, 1 NaH_2PO_4, 11 glucose, 2.5 $CaCl_2$] containing 100μM glycine for 30 min at 37°C and then fixed in ice-cold 4% paraformaldehyde/4% sucrose in PBS for 20 min, followed by ice-cold methanol for 10 minutes, then rinsed in PBS and processed for immunocytochemistry. Control coverslips were incubated in aCSF containing glycine and 200μM DL-APV.

DHPG-induced cLTD

DHPG Experiments were performed 2-3 days after transfection (at DIV 22-25). Coverslips were transferred to artificial cerebrospinal fluid [aCSF + $MgCl_2$, containing (in mM): 125 NaCl, 2.5 KCl, 26.2 $NaHCO_3$, 1 NaH_2PO_4, 11 glucose, 2.5 $CaCl_2$, and 1.25 $MgCl_2$] containing 50μM *(RS)*-3,5-dihydroxyphenylglycine (DHPG) and 200μm DL-APV for 30 min at 37°C. Control coverslips were incubated in aCSF + $MgCl_2$ containing 200μm DL-APV and no DHPG.

Immunocytochemistry and image analysis

Fixed cells on coverslips were permeabilized and blocked simultaneously in PBS containing 0.25% Triton X-100 and 10% normal goat serum (NGS) for 1 hr at room temperature. Primary antibodies (guinea pig α-GFP, guinea pig α-stargazin, rabbit α-stargazin, and mouse α-PSD-95, all diluted 1:1000 for fluorescence imaging, or 1:500 for confocal imaging) in PBS with 0.1% Triton X-100 (PBST) were then added and incubated for 2 hr at room temperature or 4°C overnight, followed by three 10-min washes in PBST. Fluorescent secondary antibodies [α-guinea pig or α-rabbit Alexa 488, α-mouse Alexa 555, and α-rabbit Alexa 647 (Invitrogen)] were diluted in PBST and added for 1hr at room temperature. After washing three more times in PBST, coverslips were mounted on slides using Fluoromount-G (Southern Biotech) and dried overnight. Fluorescent images of COS-7 cells were acquired with a 63x oil-immersion objective (NA=1.4) on a Zeiss Axiovert 200M inverted microscope using Axiovision software (Zeiss). Fluorescent images of neurons were acquired using a 63x oil-immersion objective (NA=1.4) affixed to a Zeiss LSM 510 confocal microscope. Z-projections (max intensity) of stacks of neuron images were made and analyses performed blind using NIH ImageJ software (http://rsb.info.nih.gov/ij/index.html). Analysis was performed on neurons that exhibited pyramidal somatic morphology, had dendritic PSD-95 clusters that could be distinguished from adjacent, untransfected neurons, and appeared healthy (lacking blebbing or dendritic discontinuity). For synaptic clustering analysis, the threshold for PSD-95-positive synaptic clusters was fixed at twice the level of background fluorescence in the underlying dendritic shaft. This threshold was selected because it was the lowest level at which visually-identifiable synaptic PSD-95 clusters were consistently isolated without picking up brighter areas in the dendritic shaft, and ensured that synaptic PSD-95 clusters were selected using the same criteria across different treatments and experimental preparations. The “Analyze Particles” function was used to create masks of PSD-95 clusters that were at least 0.1μm^2 in size, and clusters that colocalized with GFP staining along a selected length of dendrite were used for analysis.

Synapse:dendritic shaft ratio (SSR) was calculated by dividing the intensity of PSD-95 or stargazin staining within a PSD-95 cluster by the average staining intensity of the underlying dendritic shaft. SSR values were normalized to the wild type stargazin control values (Figure 3) or to the proper stargazin mutant control values (Figures 4-5 and Tables 1-2) within each experiment to account for staining variability across experiments. The cLTP and cLTD experiments were repeated four times each using different neuronal culture preparations. Sample size *n* refers to the number of cells that were analyzed. All results are reported as mean ± SEM. Statistical differences of the means were determined using Student's *t*-test for independent samples when comparing two samples, and one-way ANOVA with post hoc Fisher's least significant difference (LSD) tests for comparing more than two samples. Results were considered significant when $p<0.05$. Statistical analyses were performed using SPSS 14.0 software.

Results

Stargazin is phosphorylated at T321 by multiple protein kinases in vitro

The amino acid sequence surrounding stargazin's PDZ ligand (-ANRRT**T**PV; T321 in bold) makes up the consensus sequences for phosphorylation of T321 by several protein kinases, including PKA and PKC (consensus sequence: R/K-x-**S/T**), CaMKII (R/K-x-x-**S/T**), and MAPKs (x-**S/T**-P), and these consensus sequences are conserved in TARPs γ-3, γ-4, and γ-8 (Figure 1A). To understand the role of stargazin PDZ ligand phosphorylation in regulating stargazin and AMPAR trafficking, we first asked which of these kinases could directly phosphorylate stargazin at T321 *in vitro*.

We purified GST-fusion proteins containing the last 40 amino acids of stargazin's C-terminal cytoplasmic tail (stargazin-c40; WT) and a mutant stargazin-c40 lacking the C-terminal PDZ ligand (Δ4) and phosphorylated them *in vitro* with purified PKA, PKC, CaMKII, ERK2, or p38 MAPK. Autoradiograms from radioactive assays (containing 200μCi/μMol γ-[^{32}P]-ATP) showed that each of the tested kinases phosphorylated the control substrate myelin basic protein (MBP), and none of the kinases phosphorylated GST protein alone (data not shown). PKA, PKC, and ERK2 all strongly phosphorylated GST-stargazin Δ4 (data not shown), indicating robust phosphorylation of the c40 fusion protein outside the PDZ ligand. This background phosphorylation precluded the use of radioactive assays to measure specific stargazin T321 phosphorylation. As such, we analyzed Western blots of the phosphorylated protein samples using a stargazin T321 phospho-specific antibody (α-stargazin pT321; see Methods). We found that the WT stargazin-c40 fusion protein was phosphorylated at T321 by PKA and by ERK2 and p38 MAPKs, but not by PKC or CaMKII (Figure 1B).

Consensus sequence mutations selectively block stargazin T321 phosphorylation by PKA or MAPKs

Chetkovich et al. (2002) described a stargazin mutation in which the arginine residues that make up the consensus sequence for T321 phosphorylation by PKA were mutated to alanine [stargazin(R318,319A); -AATTPV; Figure 1C], and showed that it blocked PKA-mediated stargazin T321 phosphorylation in heterologous cells. We tested whether the R318,319A

mutation specifically blocked PKA-mediated T321 phosphorylation by introducing this mutation into GST-stargazin-c40 proteins and phosphorylated them *in vitro* with PKA and MAPKs ERK2 and p38. As expected, the R318,319A mutation blocked stargazin T321 phosphorylation by PKA, but both ERK2 and p38 MAPK were still able to phosphorylate the site (Figure 1D). We created another mutant stargazin protein in which the proline residue critical for MAPK-mediated T321 phosphorylation was mutated to alanine [stargazin(P322A); -RRTTAV; Figure 1C] and performed the same *in vitro* phosphorylation tests. The P322A mutation completely blocked stargazin T321 phosphorylation by ERK2 and p38 MAPKs, but did not affect T321 phosphorylation by PKA (Figure 1D). These results demonstrate that mutations of the minimal consensus sequences for stargazin PDZ ligand phosphorylation can specifically block phosphorylation of T321 by either PKA or MAPKs.

Stargazin phosphorylation-deficient mutants bind to PSD-95

Deletion or mutation of PDZ ligand residues that are critical for binding to PSD-95 prevents the synaptic delivery of both stargazin and associated AMPARs (Chen et al. 2000; Schnell et al. 2002; Bats et al. 2007). In order for the R318,319A and P322A mutants to be useful in probing the specific role of stargazin PDZ ligand phosphorylation in neurons, their interaction with PSD-95 must not be compromised. We therefore verified that both mutants interact with PSD-95 by assessing co-clustering and coimmunoprecipitation (coIP) of stargazin and PSD-95 in COS-7 cells.

Wild type stargazin interacts and forms clusters with PSD-95 when the two proteins are overexpressed in COS-7 cells (Chetkovich et al. 2002). To test whether the phosphorylation-deficient stargazin mutants interact with PSD-95, we introduced the R318,319A and P322A mutations into full-length stargazin proteins and overexpressed them in COS-7 cells with PSD-95. Like the wild type stargazin protein (WT), both the R318,319A and P322A mutant proteins clustered with PSD-95 (Figure 2A, C-D), but stargazin(Δ4) and a mutant protein that mimics T321 phosphorylation (T321E) did not (Figure 2B,E). Additionally, PSD-95 coimmunoprecipitated from COS-7 cell extracts with wild type stargazin and with both the R318,319A and P322A mutants, but not with the Δ4 or T321E mutants (Figure 2F). We analyzed the results of the coIP assays (n=5 experiments) by comparing the amount of PSD-95 that was pulled down by each stargazin protein to the amount of stargazin that was immunoprecipitated in the same sample (Figure 2G). An ANOVA revealed a significant effect of stargazin constructs on the amount of coIP'ed PSD-95 ($F[4,20]=4.079$, $p=0.014$), and post hoc Fisher's LSD tests showed that both stargazin Δ4 and T321E prevented the coIP of PSD-95 as compared to WT stargazin (relative intensity of PSD-95/stargazin in extracts from cells expressing WT: 1.43±0.33; Δ4: 0.04±0.04, $p=0.029$; T321E: 0.15±0.11, $p=0.043$). The amount of PSD-95 coIP'ed by either the R318,319A or P322A stargazin proteins was not different than WT (R318,319A: 1.52±0.77, $p=0.88$; P322A: 1.87±0.40, $p=0.47$). These results confirm that the mutations that block stargazin T321 phosphorylation by either PKA or MAPKs do not interfere with the stargazin's ability to interact with its synaptic scaffold, PSD-95.

Overexpression of stargazin PDZ ligand mutants in hippocampal neuron cultures

We examined stargazin clustering at PSD-95-labeled synapses in hippocampal neurons expressing wild type (WT, *n*=27) or mutant stargazin constructs (Δ4, *n*=23; R318,319A, *n*=26; P322A, *n*=22) under control conditions. Because our rabbit α-stargazin antibody (see Methods) detected overexpressed stargazin, but was not sensitive enough to detect endogenous stargazin (non-transfected neurons did not stain for stargazin; data not shown), it was ideal for studying the distribution of the overexpressed proteins. An ANOVA showed no differences between groups in the average size of PSD-95 clusters (in μm^2: WT 0.23±0.010; Δ4 0.24±0.015; R318,319A 0.24±0.009; P322A 0.25±0.013; F[3,94]=0.45, *p*=0.72; Figure 3B), PSD-95 cluster density (clusters per 10μm: WT 2.76±0.25; Δ4 2.86±0.28; R318,319A 3.35±0.24; P322A 2.80±0.30; F[3,94]=1.11, *p*=0.35; Figure 3C), or normalized PSD-95 synaptic:dendritic shaft staining ratio (SSR; WT: 100.0±4.1%; Δ4: 90.9±8.0%; R318,319A: 114.3±10.7%; P322A: 109.3±6.6%; F[3,94]=1.73, *p*=0.17; Figure 3D). An ANOVA revealed a significant interaction between stargazin construct and normalized stargazin SSR (F[3,94]=3.10; *p*=0.03). A post hoc Fisher's LSD test indicated that stargazin SSR was significantly elevated in cells expressing the stargazin(R318,319A) construct (121.1±9.6% compared to WT: 100.0±4.1%; *p*=0.029), but the Δ4 and P322A mutants were no different than wild type (Δ4: 96.3±5.8%, *p*=0.70; P322A: 94.9±7.4%, *p*=0.61, compared to WT; Figure 3E).

Chemical-LTP increases stargazin synaptic expression and requires T321 phosphorylation by PKA

Acute withdrawal from chronic APV treatment (APV withdrawal; APV-WD) induces a form of cLTP in cultured hippocampal neurons that includes an enhancement of AMPA EPSCs and increased clustering of synaptic AMPARs (Liao et al. 2001; Lu et al. 2001). Because stargazin is an integral component of mature AMPARs, we asked whether stargazin distribution is changed after APV-WD, and found that the SSR of WT stargazin is increased (APV-WD 127.3±5.4% of control; *n*=10-11 $p<0.001$, Student's *t*-test; Figure 4A), indicating increased stargazin trafficking to the synapse in cLTP. As expected, in neurons expressing the stargazin(Δ4) mutant (which lacks a PDZ ligand and does not bind to PSD-95) there was no increase in stargazin SSR after APV withdrawal (APV-WD 103.4±4.2% of control; *n*=9-11, *p*=0.72; Figure 4B). On the other hand, the stargazin(P322A) mutant, which cannot be phosphorylated at T321 by MAPKs, showed an increase in stargazin SSR following APV-WD that was comparable to that seen with wild type stargazin (APV-WD 127.0±7.7% of control; *n*=8-10, *p*=0.006; Figure 4D), suggesting that phosphorylation by MAPKs is not required for the increase in stargazin synaptic expression in LTP. In contrast, the stargazin (R318,319A) mutant, which cannot be phosphorylated at T321 by PKA, showed no change in stargazin SSR (APV-WD 98.8±6.8% APV-WD of control; *n*=8-11, *p*=0.89; Figure 4C), indicating that PKA-mediated T321 phosphorylation is required for the increase in stargazin synaptic expression in cLTP. We did not find any significant differences in PSD-95 cluster size, density or SSR after APV withdrawal for any of the stargazin constructs (Table 1).

Chemical-LTD decreases stargazin synaptic expression, and requires T321 phosphorylation by a MAPK

We observed that the survival and health (maintenance of normal anatomy) of dissociated hippocampal neuron preparations up to ~25 DIV was dramatically improved when the cultures were chronically treated with APV as opposed to being maintained in standard Neurobasal feeding media (data not shown). However, chronic blockade of NMDARs precluded the use of NMDA-induced cLTD for our studies. Another form of cLTD can be induced in the presence of APV by incubating dissociated hippocampal neuron cultures in the group I mGluR agonist *(RS)*-3,5-dihydroxyphenylglycine (DHPG). This mGluR-dependent cLTD causes a rapid dissociation of AMPARs from the synapse (Palmer et al. 1997; Xiao et al. 2001) and requires activation of MAPKs (Gallagher et al. 2004; Huang et al. 2004), much like the requirement for p38 MAPK activation for the removal of synaptic AMPARs in NMDAR-dependent LTD (Zhu et al. 2002). Because both NMDAR-dependent and -independent LTD involve MAPK-mediated decreases in synaptic AMPAR content, we reasoned that DHPG treatment was a suitable model for probing the role of stargazin PDZ ligand phosphorylation in LTD.

We found that application of 50μm DHPG for 30 minutes led to a decrease in stargazin SSR in hippocampal neurons expressing wild type stargazin (DHPG-treated cells 75.8±3.8% of control; n=11-16, p=0.004; Figure 5A). As with the cLTP experiments, stargazin(Δ4) showed no activity-dependent change in synaptic clustering following DHPG-treatment (DHPG 107.0±7.7% of control; n=11-12, p=0.45; Figure 5B). In cells expressing stargazin(R318,319A) that were treated with DHPG, stargazin SSR was decreased (DHPG 65.6±4.5% of control; n=15-18, p=0.002; Figure 5C), suggesting that stargazin T321 phosphorylation by PKA is not required for its removal from synapses in response to DHPG. Stargazin(P322A), on the other hand, was not downregulated from synapses following DHPG treatment (DHPG 107.3±11.9% of control; n=12-15, p=0.67; Figure 5D). These data suggest that MAPK-mediated stargazin T321 phosphorylation is required for the removal of synaptic stargazin in cLTD. We did not see any changes in PSD-95 cluster size or density or PSD-95 SSR as a result of DHPG treatment (Table 2).

Discussion

Stargazin controls the trafficking of AMPA receptors by two distinct mechanisms. First, stargazin promotes the cell surface expression of AMPARs independent of its interaction with PSD-95. Second, interaction of the C-terminal PDZ ligand of stargazin with PSD-95 stabilizes laterally-diffusing cell surface AMPARs at synaptic sites (Chen et al. 2000; Bats et al. 2007). The T321 residue in stargazin's PDZ ligand is a substrate for phosphorylation, and phosphorylation of this site disrupts the interaction between stargazin and PSD-95 (Chetkovich et al. 2002; Choi et al. 2002). In this study, we examined the role that PDZ ligand phosphorylation plays in regulating stargazin trafficking in synaptic plasticity.

Previous studies showed that phosphorylation of stargazin at T321 in the PDZ ligand is dramatically increased when stargazin is overexpressed with a catalytically active form of PKA in heterologous cells, and that phosphorylation of this site disrupts stargazin's interaction with PSD-95 and prevents the synaptic delivery of AMPARs (Chetkovich et al.

2002; Choi et al. 2002). We extended these findings to show that purified PKA directly phosphorylates stargazin at T321 *in vitro*. We also found that MAPKs – in particular ERK2 and p38 MAPK – can directly phosphorylate stargazin at T321, suggesting that the synaptic anchoring of AMPARs by stargazin may also be regulated by MAPKs.

In order to determine the role of stargazin T321 phosphorylation in neurons, we developed an assay using stargazin proteins containing mutations that specifically block either PKA- or MAPK-mediated T321 phosphorylation. While LTP and the associated increase in synaptic AMPAR content has been shown to be dependent on the activation of PKA and ERK2 (Matthies and Reymann 1993; English and Sweatt 1997; Wu et al. 1999; Zhu et al. 2002), and the removal of synaptic AMPARs in LTD requires ERK2 or p38 MAPKs (Zhu et al. 2002; Gallagher et al. 2004; Qin et al. 2005; Ito-Ishida et al. 2006; Moult et al. 2008), the broad inhibition of kinases using cell-permeable inhibitors affects all of the substrates of a given kinase, making it difficult to determine the importance of any one substrate in these processes. By overexpressing phosphorylation-deficient stargazin mutant proteins in dissociated hippocampal neuron cultures, we were able to assess the role of PKA- or MAPK-mediated stargazin T321 phosphorylation independently in regards to their roles in controlling the basal and activity-dependent regulation of stargazin synaptic expression.

We found that synaptic expression of the stargazin(R318,319A) mutant, which cannot be phosphorylated at T321 by PKA, was elevated under control conditions, while the basal synaptic expression of stargazin(P322A) and stargazin(Δ4) were not different than wild type. It should be noted that stargazin(Δ4), which does not bind to PSD-95, is typically diffusely localized, while the wild type protein is enriched at synapses [see for example Schnell et al. (2002)]. Our data did not reflect a decrease in the SSR of the Δ4 protein, but this might be explained by differences in experimental preparation. Our studies were performed in dissociated hippocampal neuron cultures, in which the synaptic enrichment of stargazin is less pronounced than in transfected or infected hippocampal slice cultures [compare the results shown in dissociated cultures by Chen et al. (2000) to those shown in slice cultures by Schnell et al. (2002)]. Moreover, our cultures were chronically treated with the NMDAR blocker APV, which increases the proportion of AMPAR-lacking silent synapses in hippocampal neuron cultures (Liao et al. 2001; Lu et al. 2001), a condition likely to decrease the basal synaptic clustering of wild type stargazin associated in complexes with AMPARs (Bats et al. 2007).

Though unable to demonstrate basal differences in the distribution of overexpressed wild type versus mutant stargazin proteins, our analysis of stargazin SSR allowed us to measure changes in the amount of stargazin clustered with its synaptic anchor, PSD-95, in response to treatments that chemically induce LTP and LTD. As would be expected for a critical auxiliary subunit, we found that the activity-dependent changes in stargazin synaptic clustering parallel reported changes in synaptic AMPAR content – namely, that synaptic stargazin content is increased in cLTP, and decreased in cLTD. Both of these processes require the phosphorylation of stargazin's PDZ ligand, but, interestingly, we found that changes in stargazin synaptic clustering in cLTP and cLTD require the ability of stargazin to be phosphorylated at T321 by different kinases.

Our results suggest that PKA-mediated stargazin T321 phosphorylation is important for the increase in synaptic stargazin content seen in APV withdrawal-induced cLTP, as this increase is not present in neurons transfected with the stargazin(R318,319A) mutant, which cannot be phosphorylated at T321 by PKA. The synaptic localization of the stargazin(P322A) mutant, on the other hand, increases during cLTP to the same extent as the wild type stargazin protein, and can be phosphorylated by PKA, but not by MAPKs. The decrease in synaptic stargazin content seen with DHPG-induced cLTP is not observed in neurons transfected with the stargazin(P322A) mutant, but remains present in neurons transfected with the stargazin(R318,319A) mutant, suggesting that the decrease in the synaptic localization in cLTD requires stargazin T321 phosphorylation by MAPKs, but not by PKA.

Perhaps the most perplexing question raised by this dual-regulation of synaptic stargazin expression is: how can stargazin PDZ ligand phosphorylation regulate both increases and decreases in the synaptic content of stargazin if PDZ ligand phosphorylation disrupts stargazin's interaction with its synaptic anchor, PSD-95? Disruption of stargazin-PSD-95 interactions by MAPKs could readily explain diminished stargazin clustering during cLTD, as MAPKs have been previously implicated in the removal of synaptic AMPARs in both NMDAR- and mGluR-dependent forms of LTD (Zhu et al. 2002; Gallagher et al. 2004; Huang et al. 2004; Moult et al. 2008). While the induction of mGluR- and NMDAR-dependent forms of LTD differ in their dependence on animal age and the stimulus protocol used, our data suggest that stargazin PDZ ligand phosphorylation by MAPKs could be a shared mechanism regulating stargazin/AMPAR trafficking in both forms of LTD (though direct examination of NMDAR-dependent cLTD will be required to confirm this possibility). It should be noted that numerous other factors have been implicated in controlling whether stargazin/AMPAR complexes are efficiently scaffolded at synapses. Whereas stargazin PDZ ligand binding to PSD-95 is critical for synaptic clustering, phosphorylation of stargazin at other sites within the C-terminus are also important for synaptic trafficking (Tomita et al. 2005). Additionally, phosphorylation events that affect the ability of AMPAR subunits to interact with synaptic scaffolding molecules are also important in controlling synaptic AMPAR clustering (Matsuda et al. 1999; Esteban et al. 2003; Boehm et al. 2006). Thus, during cLTD MAPK-mediated stargazin T321 phosphorylation may act to “loosen” synaptically-anchored stargazin/AMPAR complexes, and coincident phosphorylation of the GluR2 C-terminus [for example by PKC (Matsuda et al. 1999), but see States et al. (2008) and Lu et al. (2009)] might further favor dissociation of the stargazin/AMPAR complex from synapses.

The requirement for PKA-mediated T321 phosphorylation in cLTP is not as conceptually straightforward as the need for MAPK-mediated T321 phosphorylation in cLTD. PKA-mediated T321 phosphorylation during LTP might release stargazin from an extrasynaptic binding partner, thereby acting in a permissive manner to allow the synaptic insertion of stargazin and associated AMPARs in LTP. In this case, to account for the fact that T321 phosphorylation prevents stargazin from binding to PSD-95, we hypothesize that 1) phosphorylation might be transient (phosphorylation to allow release from extrasynaptic partner could be followed by dephosphorylation to permit association with PSD-95 at synapses), or 2) the synaptic anchoring of stargazin/AMPAR complexes during LTP could

rely on non-PDZ ligand protein interactions (such as those with the long-tail GluR1 AMPAR subunit).

Alternatively, the failure of stargazin(R318,319A) clustering to be upregulated at synapses during cLTP might result from saturation of synaptic scaffolding sites preventing activity-dependent increases in clustering. In this scenario, basal PKA-mediated T321 phosphorylation might be important for the removal of stargazin/AMPAR complexes from synapses during the activity-independent constitutive cycling of AMPARs. Thus, in cells transfected with stargazin(R318,319A), the stargazin/AMPAR complexes might not be properly recycled and would be effectively "stuck" at the synapse, preventing the scaffolding of new receptors during LTP. This mechanism could explain modest but significant increases in baseline stargazin clustering in cells expressing stargazin(R318,319A) as compared with cells expressing wild type stargazin.

In summary, our data suggest a novel role for stargazin PDZ ligand phosphorylation in controlling the synaptic clustering of stargazin, wherein phosphorylation by PKA and MAPKs are critical for bidirectional changes in synaptic clustering during synaptic plasticity. Although the specific protein-protein interactions affected by PKA- or MAPK-mediated stargazin phosphorylation are still unknown, we present a model in which stargazin-interactions with PSD-95 could play a central role. Because stargazin and AMPARs diffuse into and out of synaptic sites as complexes and not separately (Bats et al. 2007), it is likely that these activity- and phosphorylation-dependent changes in the synaptic clustering of stargazin reflect similar changes in the synaptic clustering of AMPARs, however, further studies are warranted to evaluate how stargazin phosphorylation affects synaptic AMPAR clustering during synaptic plasticity.

Supplementary Material

Refer to Web version on PubMed Central for supplementary material.

Acknowledgments

This research was supported by grants from the NIH (1K02NS05595) and Autism Speaks (2006-1393) to D.M.C. We thank Drs. Won Jun Choi and Amy Gamelli for critical reading of the manuscript and Andrey Popov for excellent technical support.

References

Bats C, Groc L, Choquet D. The Interaction between Stargazin and PSD-95 Regulates AMPA Receptor Surface Trafficking. Neuron. 2007; 53:719–734. [PubMed: 17329211]

Boehm J, Kang MG, Johnson RC, Esteban J, Huganir RL, Malinow R. Synaptic Incorporation of AMPA Receptors during LTP Is Controlled by a PKC Phosphorylation Site on GluR1. Neuron. 2006; 51:213–225. [PubMed: 16846856]

Carroll RC, Lissin DV, Zastrow Mv, Nicoll RA, Malenka RC. Rapid redistribution of glutamate receptors contributes to long-term depression in hippocampal cultures. Nat Neurosci. 1999; 2:454–460. [PubMed: 10321250]

Chen L, Chetkovich DM, Petralia RS, Sweeney NT, Kawasaki Y, Wenthold RJ, Bredt DS, Nicoll RA. Stargazin regulates synaptic targeting of AMPA receptors by two distinct mechanisms. Nature. 2000; 408:936–943. [PubMed: 11140673]

Chetkovich DM, Chen L, Stocker TJ, Nicoll RA, Bredt DS. Phosphorylation of the Postsynaptic Density-95 (PSD-95)/Discs Large/Zona Occludens-1 Binding Site of Stargazin Regulates Binding to PSD-95 and Synaptic Targeting of AMPA Receptors. J Neurosci. 2002; 22:5791–5796. [PubMed: 12122038]

Choi J, Ko J, Park E, Lee JR, Yoon J, Lim S, Kim E. Phosphorylation of Stargazin by Protein Kinase A Regulates Its Interaction with PSD-95. J Biol Chem. 2002; 277:12359–12363. [PubMed: 11805122]

El-Husseini AED, Schnell E, Chetkovich DM, Nicoll RA, Bredt DS. PSD-95 Involvement in Maturation of Excitatory Synapses. Science. 2000; 290:1364–1368. [PubMed: 11082065]

English JD, Sweatt JD. A Requirement for the Mitogen-activated Protein Kinase Cascade in Hippocampal Long Term Potentiation. J Biol Chem. 1997; 272:19103–19106. [PubMed: 9235897]

Esteban JA, Shi SH, Wilson C, Nuriya M, Huganir RL, Malinow R. PKA phosphorylation of AMPA receptor subunits controls synaptic trafficking underlying plasticity. Nat Neurosci. 2003; 6:136–143. [PubMed: 12536214]

Gallagher SM, Daly CA, Bear MF, Huber KM. Extracellular Signal-Regulated Protein Kinase Activation Is Required for Metabotropic Glutamate Receptor-Dependent Long-Term Depression in Hippocampal Area CA1. J Neurosci. 2004; 24:4859–4864. [PubMed: 15152046]

Huang CC, You JL, Wu MY, Hsu KS. Rap1-induced p38 Mitogen-activated Protein Kinase Activation Facilitates AMPA Receptor Trafficking via the GDI-Rab5 Complex: POTENTIAL ROLE IN (S)-3,5-DIHYDROXYPHENYLGLYCINE-INDUCED LONG TERM DEPRESSION. J Biol Chem. 2004; 279:12286–12292. [PubMed: 14709549]

Ito-Ishida A, Kakegawa W, Yuzaki M. ERK1/2 but not p38 MAP kinase is essential for the long-term depression in mouse cerebellar slices. Eur J Neurosci. 2006; 24:1617–1622. [PubMed: 17004925]

Liao D, Scannevin RH, Huganir R. Activation of Silent Synapses by Rapid Activity-Dependent Synaptic Recruitment of AMPA Receptors. J Neurosci. 2001; 21:6008–6017. [PubMed: 11487624]

Lu WY, Man HY, Ju W, Trimble WS, MacDonald JF, Wang YT. Activation of Synaptic NMDA Receptors Induces Membrane Insertion of New AMPA Receptors and LTP in Cultured Hippocampal Neurons. Neuron. 2001; 29:243–254. [PubMed: 11182095]

Lu W, Shi Y, Jackson AC, Bjorgan K, During MJ, Sprengel R, Seeburg PH, Nicoll RA. Subunit Composition of Synaptic AMPA Receptors Revealed by a Single-Cell Genetic Approach. Neuron. 2009; 62:254–268. [PubMed: 19409270]

Lüscher C, Xia H, Beattie EC, Carroll RC, von Zastrow M, Malenka RC, Nicoll RA. Role of AMPA Receptor Cycling in Synaptic Transmission and Plasticity. Neuron. 1999; 24:649–658. [PubMed: 10595516]

Lüthi A, Chittajallu R, Duprat F, Palmer MJ, Benke TA, Kidd FL, Henley JM, Isaac JTR, Collingridge GL. Hippocampal LTD Expression Involves a Pool of AMPARs Regulated by the NSF-GluR2 Interaction. Neuron. 1999; 24:389–399. [PubMed: 10571232]

Man HY, Lin JW, Ju WH, Ahmadian G, Liu L, Becker LE, Sheng M, Wang YT. Regulation of AMPA Receptor-Mediated Synaptic Transmission by Clathrin-Dependent Receptor Internalization. Neuron. 2000; 25:649–662. [PubMed: 10774732]

Matsuda S, Mikawa S, Hirai H. Phosphorylation of Serine-880 in GluR2 by Protein Kinase C Prevents Its C Terminus from Binding with Glutamate Receptor-Interacting Protein. J Neurochem. 1999; 73:1765–1768. [PubMed: 10501226]

Matthies H, Reymann KG. Protein kinase A inhibitors prevent the maintenance of hippocampal long-term potentiation. Neuroreport. 1993; 4:712–714. [PubMed: 8347813]

Moult PR, Correa SAL, Collingridge GL, Fitzjohn SM, Bashir ZI. Co-activation of p38 mitogen-activated protein kinase and protein tyrosine phosphatase underlies metabotropic glutamate receptor-dependent long-term depression. J Physiol. 2008; 586:2499–2510. [PubMed: 18356198]

Nicoll RA, Tomita S, Bredt DS. Auxiliary Subunits Assist AMPA-Type Glutamate Receptors. Science. 2006; 311:1253–1256. [PubMed: 16513974]

Nosyreva ED, Huber KM. Developmental Switch in Synaptic Mechanisms of Hippocampal Metabotropic Glutamate Receptor-Dependent Long-Term Depression. J Neurosci. 2005; 25:2992–3001. [PubMed: 15772359]

Palmer MJ, Irving AJ, Seabrook GR, Jane DE, Collingridge GL. The group I mGlu receptor agonist DHPG induces a novel form of LTD in the CA1 region of the hippocampus. Neuropharmacology. 1997; 36:1517–1532. [PubMed: 9517422]

Passafaro M, Piëch V, Sheng M. Subunit-specific temporal and spatial patterns of AMPA receptor exocytosis in hippocampal neurons. Nat Neurosci. 2001; 4:917–926. [PubMed: 11528423]

Piccini A, Malinow R. Critical Postsynaptic Density 95/Disc Large/Zonula Occludens-1 Interactions by Glutamate Receptor 1 (GluR1) and GluR2 Required at Different Subcellular Sites. J Neurosci. 2002; 22:5387–5392. [PubMed: 12097490]

Qin Y, Zhu Y, Baumgart JP, Stornetta RL, Seidenman K, Mack V, van Aelst L, Zhu JJ. State-dependent Ras signaling and AMPA receptor trafficking. Genes Dev. 2005; 19:2000–2015. [PubMed: 16107614]

Schnell E, Sizemore M, Karimzadegan S, Chen L, Bredt DS, Nicoll RA. Direct interactions between PSD-95 and stargazin control synaptic AMPA receptor number. PNAS. 2002; 99:13902–13907. [PubMed: 12359873]

Shi SH, Hayashi Y, Esteban JA, Malinow R. Subunit-Specific Rules Governing AMPA Receptor Trafficking to Synapses in Hippocampal Pyramidal Neurons. Cell. 2001; 105:331–343. [PubMed: 11348590]

Shi SH, Hayashi Y, Petralia RS, Zaman SH, Wenthold RJ, Svoboda K, Malinow R. Rapid Spine Delivery and Redistribution of AMPA Receptors After Synaptic NMDA Receptor Activation. Science. 1999; 284:1811–1816. [PubMed: 10364548]

States BA, Khatri L, Ziff EB. Stable synaptic retention of serine-880-phosphorylated GluR2 in hippocampal neurons. Mol Cell Neurosci. 2008; 38:189–202. [PubMed: 18417360]

Tomita S, Stein V, Stocker TJ, Nicoll RA, Bredt DS. Bidirectional Synaptic Plasticity Regulated by Phosphorylation of Stargazin-like TARPs. Neuron. 2005; 45:269–277. [PubMed: 15664178]

Tomita S, Chen L, Kawasaki Y, Petralia RS, Wenthold RJ, Nicoll RA, Bredt DS. Functional studies and distribution define a family of transmembrane AMPA receptor regulatory proteins. J Cell Biol. 2003; 161:805–816. [PubMed: 12771129]

Vandenberghe W, Nicoll RA, Bredt DS. Stargazin is an AMPA receptor auxiliary subunit. PNAS. 2005; 102:485–490. [PubMed: 15630087]

Wu SP, Lu KT, Chang WC, Gean PW. Involvement of mitogen-activated protein kinase in hippocampal long-term potentiation. J Biomed Sci. 1999; 6:409–417. [PubMed: 10545776]

Xiao MY, Zhou Q, Nicoll RA. Metabotropic glutamate receptor activation causes a rapid redistribution of AMPA receptors. Neuropharmacology. 2001; 41:664–671. [PubMed: 11640920]

Zhu JJ, Qin Y, Zhao M, Van Aelst L, Malinow R. Ras and Rap Control AMPA Receptor Trafficking during Synaptic Plasticity. Cell. 2002; 110:443–455. [PubMed: 12202034]

Ziff EB. TARPs and the AMPA Receptor Trafficking Paradox. Neuron. 2007; 53:627–633. [PubMed: 17329203]

Abbreviations used

AMPAR	α-amino-3-hydroxy-5-methyl-4-isoxazole propionic acid receptor
mGluR	metabotropic glutamate receptor
PDZ	PSD-95/Dlg/ZO-1
PSD-95	postsynaptic density-95
TARP	transmembrane AMPAR regulatory proteins
GFP	green fluorescent protein
LTP	long-term potentiation
cLTP	chemically-induced LTP

LTD	long-term depression
cLTD	chemically-induced LTD
APV	D,L-aminophosphonovalerate
DHPG	(*RS*)-3,5-dihydroxyphenylglycine

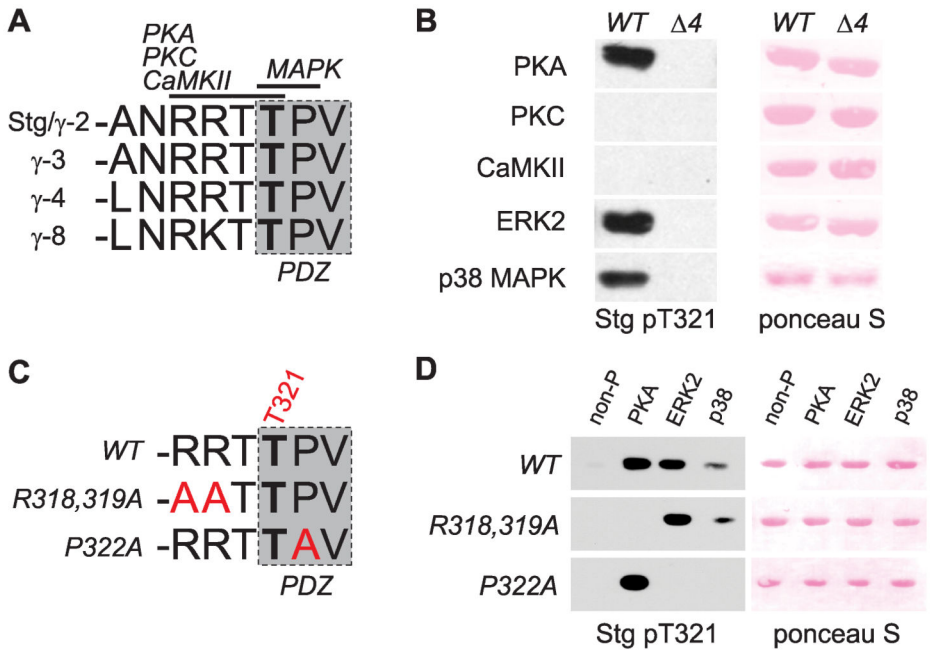

Figure 1.

Stargazin is phosphorylated at T321 by multiple protein kinases *in vitro*. *A*. The C-termini of stargazin-like TARPs (stargazin/γ-2, γ-3, γ-4, and γ-8) contain a conserved type-I PDZ ligand (shaded box). A critical threonine residue within the PDZ ligand (corresponding to T321 of stargazin; bold) is surrounded by consensus sequences for phosphorylation by PKA, PKC, CaMKII, and MAPKs (including ERK1/2 and p38 MAPK) as indicated. *B*. Western blotting to detect stargazin phosphorylated at T321 shows that a GST fusion protein containing the stargazin C-terminal 40 (c40) amino acids (WT) is phosphorylated at T321 *in vitro* by PKA and the MAPKs ERK2 and p38, but not by PKC or CaMKII. A similar fusion protein lacking the last 4 amino acids (Δ4) is not phosphorylated. *C*. Consensus sequence mutations (red text) are designed to specifically block T321 phosphorylation by PKA (R318,319A mutation) or MAPKs (P322A mutation). *D*. Western blotting to detect stargazin phosphorylated at T321 shows that although stargazin c40 is phosphorylated by PKA, ERK, and p38 MAPK, indicated mutations in stargazin c40 GST-fusion proteins (R318,319A mutation or P322A) specifically block phosphorylation (by PKA or MAPKs, respectively).

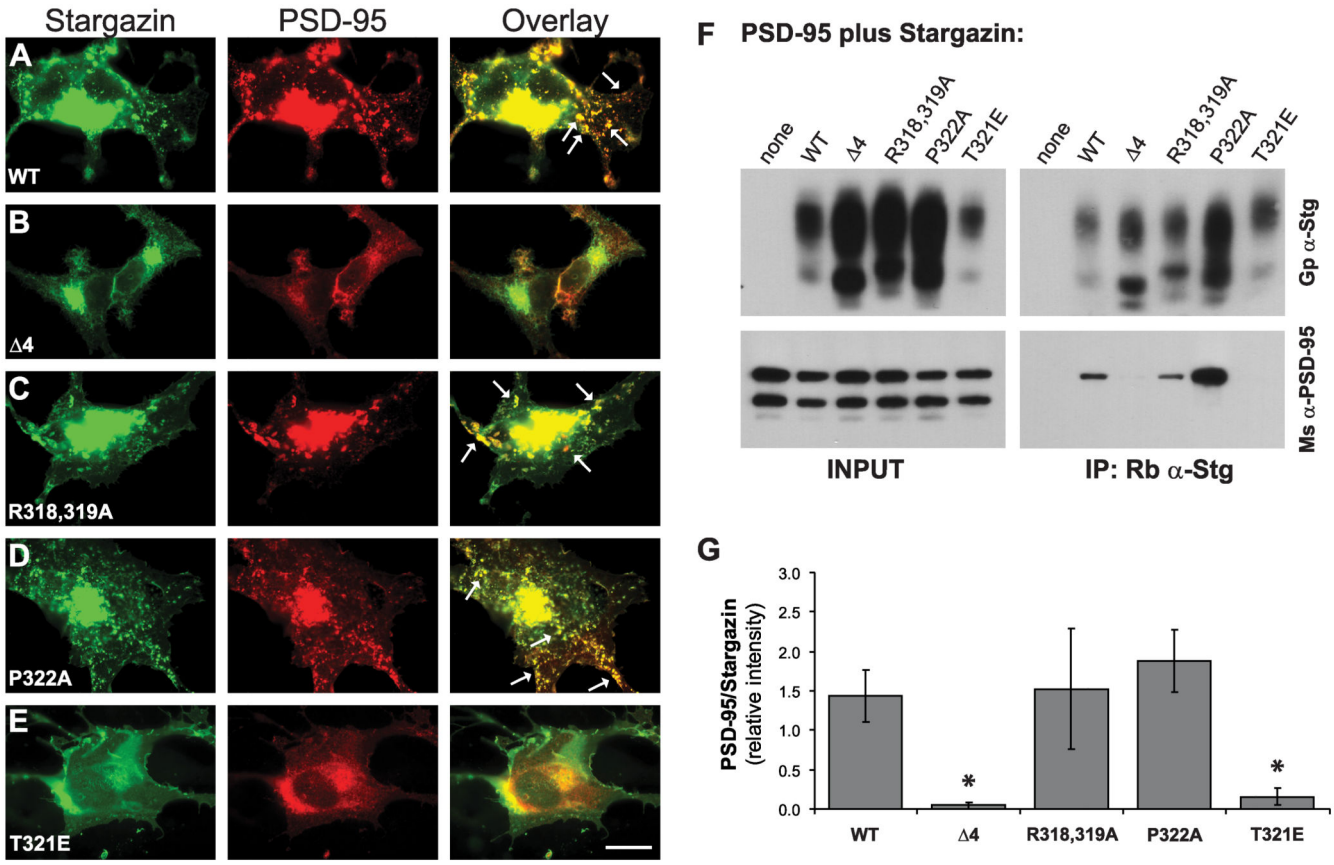

Figure 2.

Stargazin phosphorylation-deficient mutants bind to PSD-95. *A-E*. Clustering of stargazin (green; left) and PSD-95 (red; center) in COS-7 cells. *A*. Wild type stargazin and PSD-95 colocalize in cell-surface clusters (overlay, right; clusters indicated with arrows) when the two proteins are coexpressed in COS-7 cells. *B,E*. Stargazin(Δ4), which lacks the C-terminal PDZ ligand, and stargazin(T321E), which mimics PDZ ligand phosphorylation, do not bind to PSD-95 and are diffusely localized in COS-7 cells. *C-D*. The stargazin(R318,319A) and stargazin(P322A), which lack PDZ ligand phosphorylation by PKA and MAPKs, respectively, cluster with PSD-95 (scale bar = 10μm). *F-G*. COS-7 cells were transfected with PSD-95 alone or with the indicated stargazin constructs. Cell lysates were prepared and stargazin was immunoprecipitated. *F*. Representative Western blots show that PSD-95 was coimmunoprecipitated with wild type stargazin, but not with stargazin(Δ4) or stargazin(T321E) PSD-95 coimmunoprecipitated with both the stargazin(R318,319A) and stargazin(P322A) mutants (bottom right), indicating that these mutant stargazin proteins bind to PSD-95. *G*. Summary of five experiments, in which the amount of coimmunoprecipitated PSD-95 was compared to the amount of immunoprecipitated stargazin in the same samples in order to quantify the relative strength of the interaction between PSD-95 and each of the stargazin proteins. Both the Δ4 and T321 mutations significantly blocked the coimmunoprecipitation (coIP) of PSD-95 with stargazin, while coIP of PSD-95 with both the R318,319A and P322A mutant proteins were no different than with the wild type protein (* $p<0.05$).

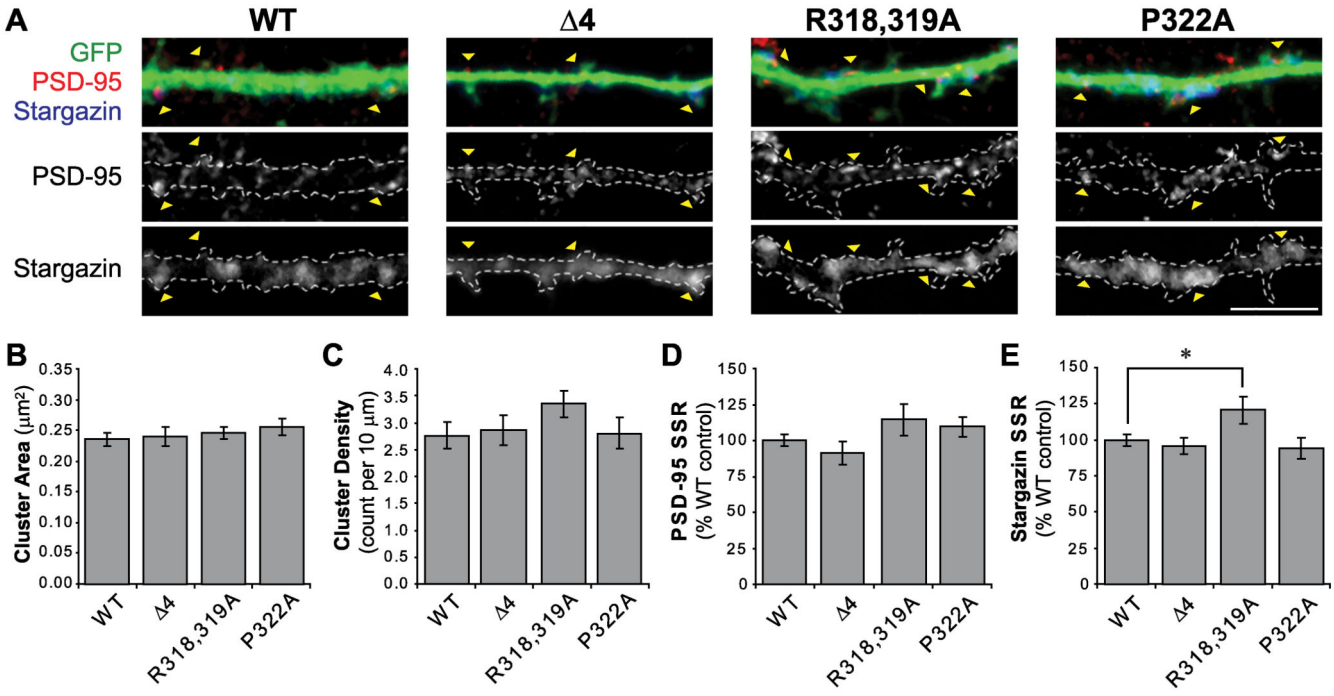

Figure 3.

Expression of stargazin mutants in hippocampal neurons. *A*. Dissociated hippocampal neuron cultures (20-22 days in vitro; DIV) were transfected with GFP and wild type (WT) or mutant stargazin constructs, as indicated. Cells were fixed 2-3 days later and stained for GFP (Gp α-GFP; green), stargazin (Rb α-stargazin; blue), and PSD-95 (Ms α-PSD-95; red). PSD-95 images were thresholded to define synaptic clusters that had a staining intensity at least twice the intensity of the underlying dendritic shaft, and clusters that colocalized with GFP were used for analysis (arrowheads). Scale bar 5μm. *B-C*. In neurons expressing the Δ4, R318,319A, or P322A stargazin mutants, the average size and density of PSD-95 clusters were not different than in cells expressing WT stargazin. *D*. The stargazin mutants also did not affect the spine:dendritic shaft staining ratio (SSR) for PSD-95 when compared with neurons expressing the WT control. *E*. Whereas the SSR of stargazin(Δ4) and stargazin(P322A) were not significantly different than WT, the SSR of stargazin(R318,319A) was elevated (* p=0.029), indicating an increase in stargazin synaptic clustering in neurons expressing stargazin(R318.319A). n=22-27 cells per group.

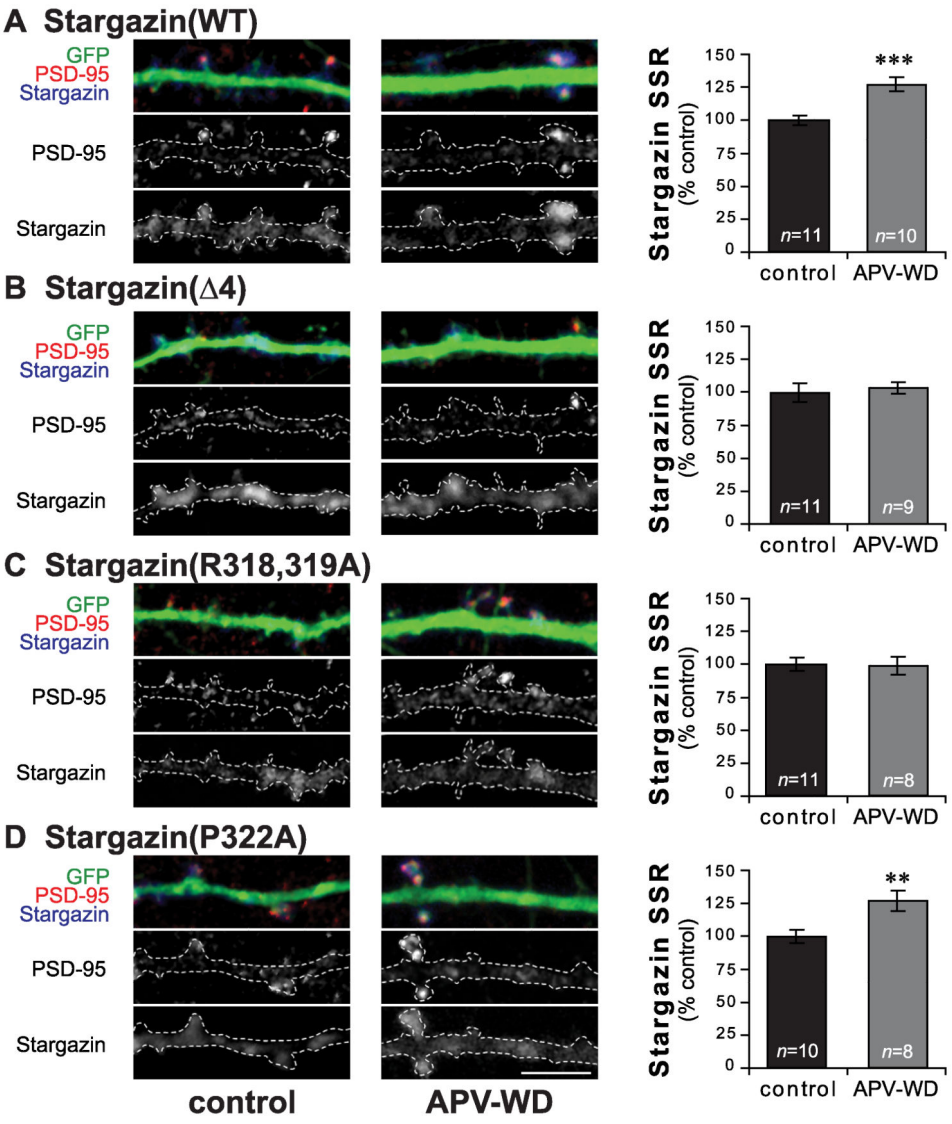

Figure 4.

APV withdrawal-induced cLTP increases stargazin synaptic clustering in a PKA-dependent manner. Hippocampal neurons were grown in media containing 200μm APV, and transfected with GFP and wild type or mutant stargazin at DIV20-22. 2-3 days after transfection, neurons were transferred to aCSF with (control; left) or without APV (APV withdrawal; middle) for 30min, then fixed and stained for GFP (Gp α-GFP; green), stargazin (Rb α-stargazin; blue), and PSD-95 (Ms α-PSD-95; red). In cells expressing wild type stargazin (WT; *A*), stargazin SSR was increased after APV withdrawal. This increase was blocked by deletion of the C-terminal stargazin PDZ ligand (Δ4; *B*). Stargazin(R318,319A), which cannot be phosphorylated at T321 by PKA, also prevents the APV withdrawal-induced increase in stargazin clustering (*C*), while stargazin(P322A), which cannot be phosphorylated at T321 by MAPKs, is similar to WT (*D*). Scale bar 5μm; ** $p < 0.01$, *** $p < 0.001$.

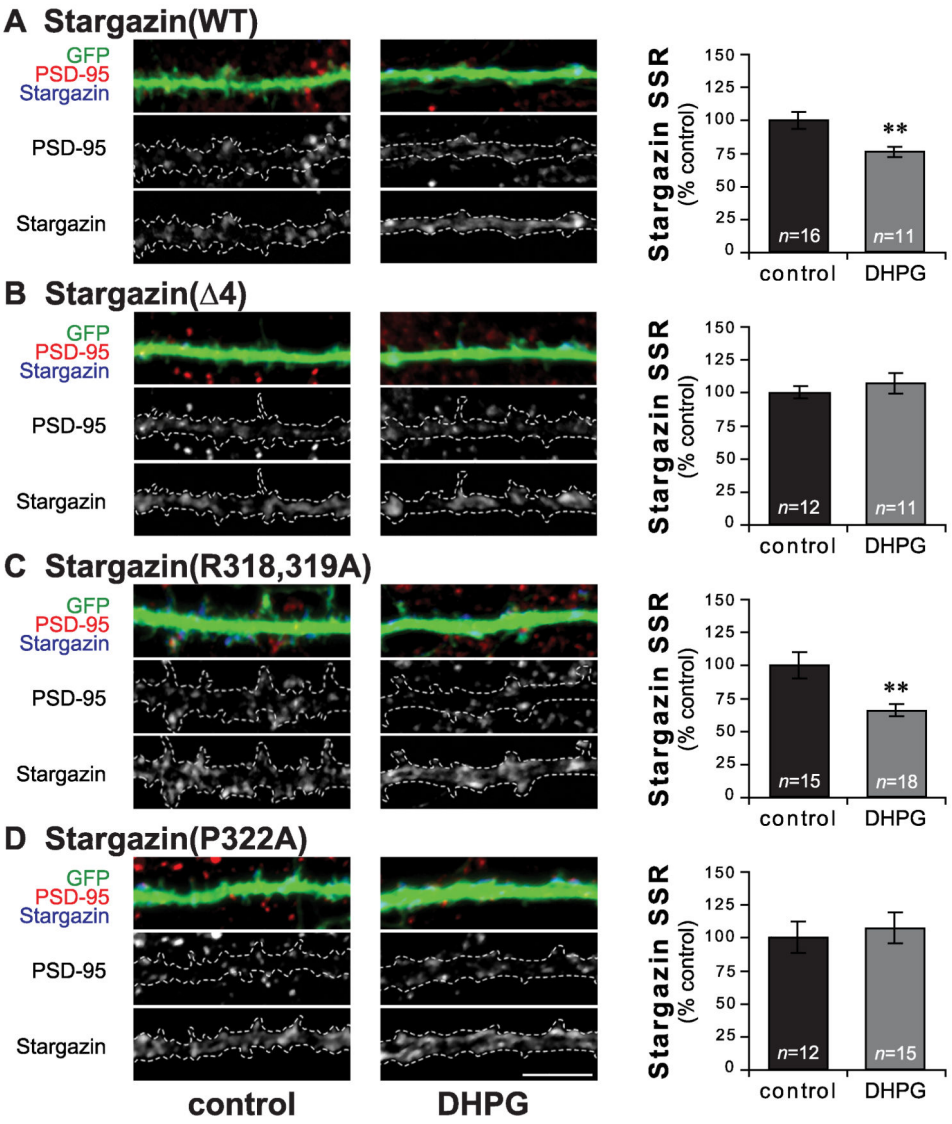

Figure 5.

DHPG-induced cLTD decreases stargazin synaptic clustering in a MAPK-dependent manner. Hippocampal neurons were grown in media containing 200μm APV, and transfected with GFP and wild type or mutant stargazin at DIV20-22. 2-3 days after transfection, neurons were transferred to aCSF without (control; left) or with 50μM DHPG (DHPG; middle) for 30min, then fixed and stained for GFP (Gp α-GFP; green), stargazin (Rb α-stargazin; blue), and PSD-95 (Ms α-PSD-95; red). In cells expressing wild type stargazin (WT; *A*), stargazin SSR was decreased after DHPG treatment. This decrease was blocked by deletion of the C-terminal stargazin PDZ ligand (Δ4; *B*). Stargazin(R318,319A), which cannot be phosphorylated at T321 by PKA, shows a decrease in stargazin SSR similar to WT after DHPG treatment (*C*), while stargazin(P322A), which cannot be phosphorylated at T321 by MAPKs, blocks the decrease in stargazin SSR (*D*). Scale bar 5μm; ** $p < 0.01$.